



HAL
open science

ABAQUS/CFD numerical investigation of an axisymmetric water jet impacting a fixed target: Theoretical validation

Ikram Ben Belgacem, L. Cheick Lotfi, W. Ben Salem Wacef

► **To cite this version:**

Ikram Ben Belgacem, L. Cheick Lotfi, W. Ben Salem Wacef. ABAQUS/CFD numerical investigation of an axisymmetric water jet impacting a fixed target: Theoretical validation. 25e Congrès Français de Mécanique, Aug 2022, Nantes, France. hal-04280051

HAL Id: hal-04280051

<https://hal.science/hal-04280051v1>

Submitted on 13 Nov 2023

HAL is a multi-disciplinary open access archive for the deposit and dissemination of scientific research documents, whether they are published or not. The documents may come from teaching and research institutions in France or abroad, or from public or private research centers.

L'archive ouverte pluridisciplinaire **HAL**, est destinée au dépôt et à la diffusion de documents scientifiques de niveau recherche, publiés ou non, émanant des établissements d'enseignement et de recherche français ou étrangers, des laboratoires publics ou privés.

ABAQUS/CFD numerical investigation of an axisymmetric water jet impacting a fixed target: Theoretical validation

L. Cheikh^{a, b}, I. Ben Belgacem^{a, *}, W. Ben Salem^a

^a Laboratoire de Génie Mécanique, Ecole Nationale d'Ingénieurs de Monastir, Université de Monastir, Tunisie

^b Institut Préparatoire aux Etudes d'Ingénieur de Monastir, Université de Monastir, Tunisie
*ikrambenbelgacem@gmail.com

Résumé :

Dans cette étude, les résultats d'une étude numérique sur les caractéristiques d'écoulement provenant d'un seul jet d'eau axisymétrique impactant une surface plane sont présentés. Le comportement du jet en dynamique des fluides computationnelle (CFD) est étudié à l'aide d'une méthode FV (volume fini) implémentée sur ABAQUS/CFD. Le jet atteint le niveau de la structure avec une vitesse initiale de 113 m/s à travers une buse d'un diamètre de 1 mm. L'obstacle est situé à 10 mm de la sortie d'eau. Le modèle K-ε est adopté pour traiter les phénomènes de turbulence. Le champ d'écoulement se compose de quatre régions distinctes ; chacun est discuté en détail. De plus, la répartition des pressions est également détaillée. Les résultats numériques sont comparés à l'étude théorique du profil de vitesse déjà présentée et validée expérimentalement dans le cadre des travaux de Martin en 1977 [1]. L'approche utilisée dans la modélisation numérique a montré un bon accord entre la théorie et les données numériques.

Abstract:

In this study, the results of a numerical survey on the flow characteristics coming from a single axisymmetric water jet impinging on a flat surface are presented. The Computational Fluid Dynamics (CFD) behavior of the jet is investigated using a FV (Finite volume) method implemented on ABAQUS/CFD. The jet hits the target with an initial velocity 113m/s through a nozzle with a diameter of 1mm. The obstacle level is located after 10mm away from the water outlet. The K-ε model is adopted to handle the turbulence phenomena. The flow field consists of four distinct regions; each one is discussed in detail. Furthermore, pressure distribution is also detailed. Numerical results are compared with theoretical survey of velocity profile already presented and experimentally validated within the work of Martin in 1977 [1]. The used approach in the numerical modelling showed a good agreement between theory and numerical data.

Keywords: Water-impacting jet, CFD, Turbulence, ABAQUS, Velocity profile, Pressure distribution, slope target

1 Introduction

The impact of a high-speed jet on an obstacle is observed in several applications starting with home uses and moving on to space technology devices. The high-speed water jet is characterized by its many advantages and by its simple industrialization [2]. The most common way to produce a high velocity stream of water is to force a quantity of water through a converging nozzle. Using this

method, the water is accelerated and the jet can reach speeds of up to 4000 m/s [3]. The technique of water jets is now applied in many industrial fields, such as welding, cleaning (turbine, engine parts), decoration process, cutting (metal sheet, plastic), material removal by abrasive water jet, the assisted high-pressure water jet [4], [5], [6], [7], [8] and [9]. The jet's velocity profile is the main term of the momentum, which will be applied to the target. Then, it is interesting to give it the greatest importance in jets studies. The pressure of the jet on the target surface is not a minor parameter either, therefore it must also be analyzed and optimized. Generally, studies of this type of flow must go through an experimental expertise. However, the implementation of instrumented tests is often time-consuming and expensive, or even impossible, as for large industrial installations, for example. In addition, the sensitivity of the observation coming from the multidisciplinary aspect of physical phenomena (speed of the process, evaporation of the lubricating fluid, the microscopic scale of stress state, etc.) makes that we rarely turn to an experimental study [8], [9] and [10]. Therefore, in order to have a qualitative and quantitative idea of the behavior of the jet before and after the impact, a numerical experiment is often carried out. Indeed, in one hand a numerical simulation gives the opportunity to test different models then judge and validate the performance of each with the benefits of avoiding the disadvantages of experimental studies. This approach cannot present all the physical aspects of the phenomenon studied. However, it allows dealing with relatively complex problems by posing fewer assumptions than an analytical approach. It can be less expensive than an experimental approach. Elsewhere numerical tests enable research to complete, understand, and define the experimental results mainly in fluid mechanics and thermal analysis. It is well known that in the field of fluid mechanics, CFD is the method that offers all the advantages previously mentioned. Thanks to its simplicity of application, it is integrated into many commercial software. From an analytical perspective, with some assumptions, the analytical approach has the advantage of providing exact solutions. The postulate of simplifying assumptions limited the scope of the approach to simple cases. Sometimes these results are quite satisfactory and indicate a good approximation of the problem. This paper is dedicated to the study of a high-pressure water jet impacting a fixed horizontal plate using the CFD implanted in the ABAQUS software. The jet leaves the nozzle at a speed of 113 m/s and it is considered turbulent. The ratio of jet height to nozzle diameter is set to 10: $H/D = 10$. The model presented within this framework treated only from a mechanical point of view. The thermal effect of the jet is not considered. However, there is few works based on direct numerical simulation to study the dynamic behavior of an impacting and axisymmetric jet. This flow configuration presents several difficulties, particularly when dealing with outlet boundary conditions. We will also show in our study that the choice of spatial discretization patterns is a crucial issue. By considering, first, a «simple» configuration, we propose to highlight the problems of a numerical order. This preliminary work will help guide our future choices regarding the discretization and boundary conditions used for numerical simulations of a machining case. The flow structure depends on many parameters such as injection conditions (Reynolds number, turbulence, etc.), impact height. The purpose of the study is to determine the influence of each of these parameters in the case of a jet orthogonally impacting a flat target.

2 THEORETICAL BACKGROUND

A simplified analytical model can be used as a guide in the numerical model. It is in this option that we propose to conduct the following analytical study. Indeed, the literature is not rich in numerical studies dealing with the problems of impacting jets handled by ABAQUS. Moreover, in the context of this paper we do not have the possibility of conducting an experimental study. To validate the modelling and to calibrate the CFD numerical approach, we will refer to the work of Holger MARTIN [1]. Dating back to 1977, this work was carried out analytically and based on an empirical

formulation. Figure 1 shows an axisymmetric impacting jet hitting a horizontal plate target. Under some conditions, technically realistic, the free jet developed from the outlet of the nozzle is generally turbulent. This turbulence is strongly related to the number of Reynolds based on the diameter. Schröder [12], Glaser [13] and other authors [14] and [15], has conducted many analytical studies in particular. These studies show that such a flow can be subdivided into 4 characteristic regions as shown in Figure 2. These regions, which will be detailed later, are the potential core, established flow, deflection (stagnation flow) and a lateral flow outside the stagnation zone. This latter region is also called the wall jet region (or parietal jet), Glauber [16].

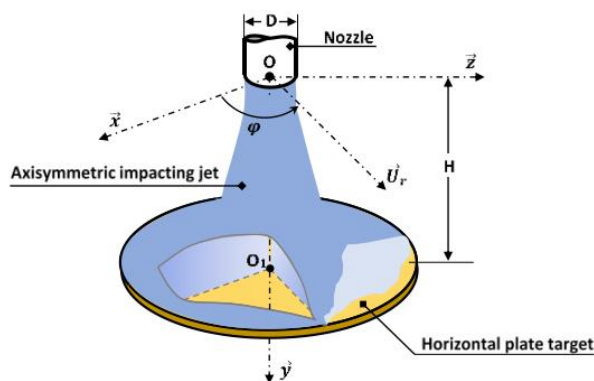


Figure 1: Simplified illustration of an axisymmetric jet impacting a fixed plane target.

Free jet zone	Zone of potential core (Region I)
	Zone of established flow (Region II)
Deflexion zone (stagnation)(Region III)	
Wall jet zone (Region IV)	

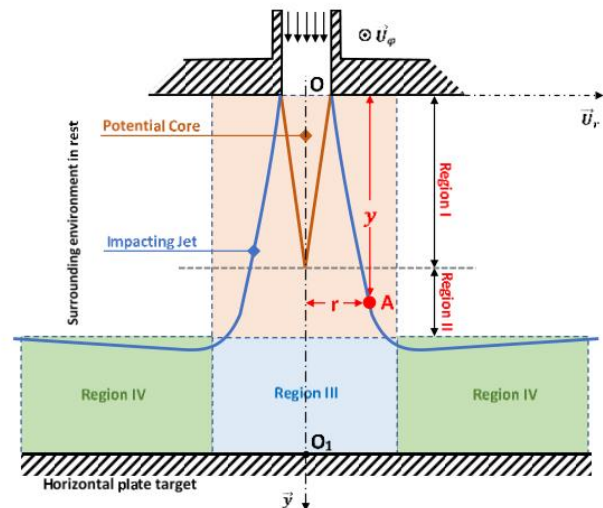


Figure 2: regions of an impacting jet.

At the outlet of the circular nozzle, the jet is similar to a free jet, except in the immediate vicinity of the impact area. Indeed, the disturbance created by a solid wall on an incident jet propagates upstream at a speed equal to the difference between the sonic speed and the speed of the fluid. Thus, the wall effect decreases with the increase in the number of Mach and disappears completely at Mach 1. The disturbance created by the wall would be unable to spread upstream. Hence, the 4 main regions forming the typical velocity profile of an impacting jet are as follow. **1) The Free jet zone (Regions I and II)**; When the fluid flows into an environment at rest, the jet is called free. Near the opening of the nozzle and due to the velocity gradient between the jet and the surrounding environment, a mixture arises and a turbulent mass exchange takes place. This mixture is characterized by a shear stresses due to the viscosity. The mixing zone grows in width in the downstream direction of the jet. leaving in its wake a potential core where the physical properties and the velocity profile of the fluid are relatively constant. This core zone dissipates gradually with the spread of the fluid. Schlichting [18] showed that at a given point $A(r, y)$ of the free stream (cf. figure 2), the radius " r " is directly proportional to the height " y ". According to reference [18], the pressure in the potential core region is practically constant. It is equal to the pressure in the surrounding environment at rest, namely atmospheric pressure. By an intensive and continuous exchange of the momentum with the surrounding environment on the free boundary, the jet widens linearly with its length " y " to a limit distance " yG " from the solid surface as presented in figure 3. The velocity profile, having almost a cylindrical shape at the near outlet of the nozzle, propagates to the free boundary. For a sufficient length of the free stream, it approaches a bell shape announcing the beginning of the stagnation zone.

A Gaussian distribution given by the following

$$V(r, y) = V(0, y) \exp\left\{-\left(\frac{r}{cy}\right)^2\right\} \quad (1)$$

The constant C in equation (1) takes a value of about 0.1: $C \approx 0.1$ [1]. It is slightly dependent on the shape of the nozzle and the Reynolds number governing the flow [1]. Equation (1) is valid only in region II. This zone, located between region I and region III as presented in figure 3, is limited in one hand by, the length of the core zone " yk ". Up to this limit, the fluid velocity on the axis remains almost constant $V(0, y) = V_e$ if $y < yk$. And, in the other hand, the distance " yG " from the boundary, which marks the limit of the stagnation zone

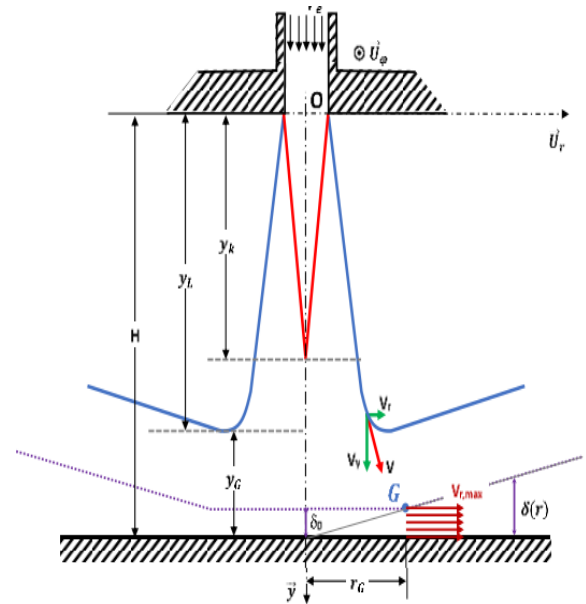


Figure 3: Velocity profile in the different characteristic regions.

For $0 \leq y \leq yG$, the velocity on the axis (O, y^{\rightarrow}) of the jet can be calculated according to Schlunder [19] by the following equation:

$$V(0, y) = V_e \sqrt{1 - \exp\left\{-\left(\frac{D}{c\sqrt{2}y}\right)^2\right\}} \quad (2)$$

Here " yk " corresponding to the toposition where the centerline velocity reaches 97% of its maximum value. Equation 2 may be reduced to the simple following equation giving the relation between onstant C and core length yk :

$$C = 0,102 \left(\frac{4D}{yk}\right) \quad (3)$$

So, the length of the core is about four times the diameter of the nozzle: $yk = 4D$. For turbulent flow, other researchers have shown that the length of the potential core area is proportional to the diameter of the nozzle: $yk \approx \sigma D$. Unfortunately, the proportionality coefficient " σ ", experimentally investigated, varies from a study to another. The observed divergence generally exceeds the expected experimental error. It is probably due to the effect of the scale choice and the turbulence intensity inside the jet. Other factors such as nozzle shape, initial velocity, etc...., seem to play an important role in the difference between experimental results. However, researchers agree that the ratio of proportionality " σ " varies between $4,7D$ and $7,7D$ [20]: $4,7D \leq yk \leq 7,7D$.

Enough away from the nozzle exit ($y \gg yk$), a simple Taylor series written around 1 of equation 2 allows us to show that it tends asymptotically towards a hyperbolic shape. Subsequently, the relation between the centerline velocity regarding the y -axis is given in the following relation

$$V(0, y) = V_e \left(\frac{D}{c\sqrt{2}y}\right) \quad (4)$$

2) Deflection Zone (Region III): According to Schrader [12], flow stagnation begins near the impact surface. He estimates that the limit distance « yG » is equal to about 1.2 times the diameter of the nozzle as mentioned in figure 3: $yG = 1,2D$. Within this area, the radial component of the jet velocity increases while the axial component decreases rapidly. As a result, a local increase in pressure is observed. The latest could be explained by the conversion of kinetic energy. The impact area is thus marked by a pressure gradient in the radial direction. Such a pressure gradient is responsible for an

increase in velocity in the same direction. The end of the stagnation zone is bounded by a radial velocity, which reaches a maximum Vr,max . The stagnation zone is roughly delimited by $rG \approx 0.5D$. Outside the boundary layer, but sufficiently close to the impact point $O1(0,H)$, the equations (5) show that the velocity components are linearly proportional to the coordinates of the stagnation point (Cf. figure 3). The boundary layer thickness δ_0 is shown in figure 3. When the ideal stagnation flow is reached, the thickness of the boundary layer becomes invariant. It no longer depends on the radius "r" in the case of a parallel flow. By neglecting the friction effect, the flow velocity in the vicinity of the stagnation point ($r = 0, y = H$) is given by the following equations:

$$\begin{cases} V_y = 2 a \tilde{y} & (a) \\ V_r = a r & (b) \end{cases} \quad (5)$$

Here: $\tilde{y} = H - y$ and « a » is a constant coefficient.

In case of real stagnation flows coming from impacting jets with finite diameter nozzle and such as $H/D \leq 10$, Schrader [12] and Dostogru [21] determined the constant "a" and the thickness "δ0". They expressed them in the following equation:

$$a = \left(\frac{V_e}{D}\right) \left(1,04 - 0,034 \frac{H}{D}\right) \quad \text{and} \quad \delta_0 = \frac{1,95 D}{\sqrt{\left(1,04 - 0,034 \frac{H}{D}\right) Re}} \quad (6)$$

Using all expressions and data presented in the work of Martin[1] we have determined the different parameters. Indeed, we will investigate the case of a nozzle with a diameter $D = 1 \text{ mm}$, placed at a height $H = 10 D = 10 \text{ mm}$ from the plate. The water is ejected from the nozzle at a velocity $Ve = 113 \text{ m/s}$. The Reynolds number is then $Re = 1.13 \cdot 10^5$. Using equation (6), then the thickness of the boundary layer is given as $\delta_0 = 6.9 \cdot 10^{-3} \text{ mm}$ as well as the constant $a = 0,7 Ve$. So, the ordinate « yG » of point G, is estimated at: $yG = 1,2 D = 1,2 \text{ mm}$. In aim to calculate rG , an additional mathematical approach is needed. Using equation 1 the velocity of the point G is presented as follows:

$$V(r_G, H) = V(0, H) \exp\left\{-\left(\frac{r_G}{C H}\right)^2\right\} \quad (7)$$

Note that $C \times H \approx 1$, then equation 7 then becomes:

$$V(r_G, H) = V(0, H) e^{-r_G^2} \quad (8)$$

At the level of the target ($y = H$), the centerline velocity is given by equation 4: $V(0, H) = VG = Ve \sqrt{2}$. By replacing, in equation 8 $V(0, H)$ by its expression, we obtain a first expression of the centerline velocity at the so-called point G as given in equation 9:

$$V(r_G, H) = V_G e^{-r_G^2} \quad (9)$$

On the other hand, equation 5.b is an additional expression to calculate the velocity of the point G as a function of the constant a. Remember that the constant has been determined above and it is worth $a = Ve \sqrt{2} = VG$. The velocity at point G is then given by equation 10 as follows:

$$V(r_G, H) = a r_G = V_G r_G \quad (10)$$

Thus, based on the continuity of the velocity profile at point G, we have equality between the velocity given respectively by equations 9 and 10. This allows deducing equation 11, which gives rG :

$$r_G = e^{-r_G^2} \quad (11)$$

Back to the Taylor series written around 1 near 0, the non-linear equation 11 is reduced to a polynomial: $rG^2 + rG - 1 = 0$. It admits as the only physically accepted solution

$$rG = 0,62 \text{ mm}$$

3) Wall jet zone (Region IV): Compared to the stagnation line ($y > yG$), this area of the stream can be subdivided into two layers: A parietal layer, between the wall and the stagnation line and an external

layer above the line. They are analogous to a wall boundary layer and a mixing layer respectively. The external layer is not a new mixing layer but it is an extension of the one coming from the free stream. It is simply modified by the target. The turbulent structures formed in the free stream region, extend radially as far as they approach the target. The interaction of these structures with each other causes the separation of the boundary layer and the emergence of other secondary turbulent structures. At the end, and because of the «finite breathing» of the jet resulting from the phenomenon of intense turbulence and the momentum exchange with its resting surrounding environment, the accelerated stagnation flow eventually turns into a decelerated wall jet flow. Thus, the radial component « V_r » of the velocity, which initially increases linearly from zero, must reach a maximum value at a certain distance rG from the stagnation point. Then, it ends up moving towards zero following a curve governed by a $r - n$ function. In the case of axial turbulent wall jets this velocity is inversely proportional to the radius r (i.e. $n = 1$) [16], [22], [23] and [1]. While the stabilizing effect of acceleration maintains the laminar boundary layer in the stagnation zone, the transition to turbulence generally occurs immediately after rG in the decelerating flow region. As a result of this analytical approach, and in terms of fluid dynamics, it is obvious that the impacting jet involves several different physical phenomena. It should be recalled again that we have excluded from this study the thermal aspects. Thus, understanding the physics of this flow and the limitations of numerical methods to reproduce it are major interests. Within this framework, we propose to explain and investigate this purpose using numerical modeling through ABAQUS/CFD

3 NUMERICAL SIMULATION

This section, dedicated to the study and calibration of the numerical CFD method. the modeling is handled using ABAQUS 6.14-1 by the "CFD" tool, specifically dedicated to fluid dynamics. The geometric configuration of the proposed jet is axisymmetric. The water flows from a nozzle with a diameter $D = 1$ mm and a distance of $H = 10 D = 10$ mm from the obstacle level. The target, subjected to the action of the jet, has a radius $r = 12 D$. Table 1 illustrates the various parameters involved in the problem. Since we propose to study an axisymmetric jet, we considered that a cylindrical volume would be the most appropriate. This choice is the result of a series of simulations testing many geometric configurations. Indeed, the studied volume is the volume that can be occupied by the fluid during the simulation. The diameter of the cylinder was fixed in aim to avoid the end-effect. In this table, we also presented the fluid volume and the adopted turbulence model. When it comes to the boundary conditions, the nozzle output velocity is equal to 113 m/s. On the rest of the upper wall of the study volume, a zero velocity is imposed. A no-slip condition is applied to the target. The lateral surface of the volume representing the output and it is assumed to be under atmospheric pressure. For the fluid modeling, the water is considered as an incompressible and homogenous fluid. The Mie-Grüneisen EOS is adopted. it is Hugoniot's linear Us-Up form, implemented in Abaqus, which is written

$$p = \frac{\rho_0 c_0^2 \eta}{(1-s \eta)^2} \left(1 - \frac{\Gamma_0 \eta}{2} \right) + \Gamma_0 \rho_0 E_m \quad (12)$$

Where: c_0 and s define the relationship between the shock velocity « U_s » and the velocity « U_p » of a particle as follows: $U_s = c_0 + sU_p$. The values of these parameters as well as the physical properties of the water were taken from the literature. Table 2 shows the different values of these parameters. The fluid flow in the current impinging jet study is turbulent due to the large Reynolds number of $Re = 113000$. Therefore, the best turbulence model used in the literature is called $k - \varepsilon$ which can be used for high Re values to deliver acceptable numerical results in a steady flow analysis for higher H/D ratios [40]. The ratio is equal to 10 in our case. We have used this model of turbulence presented in ABAQUS to handle this phenomenon.

Table 1 : Formulation of the impacting jet problem: The CFD model parameters.

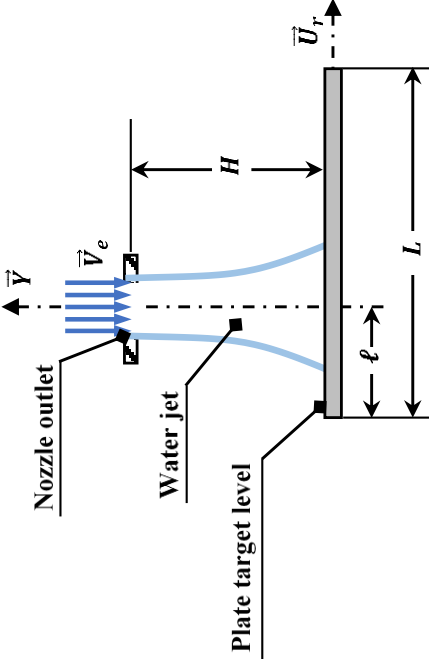
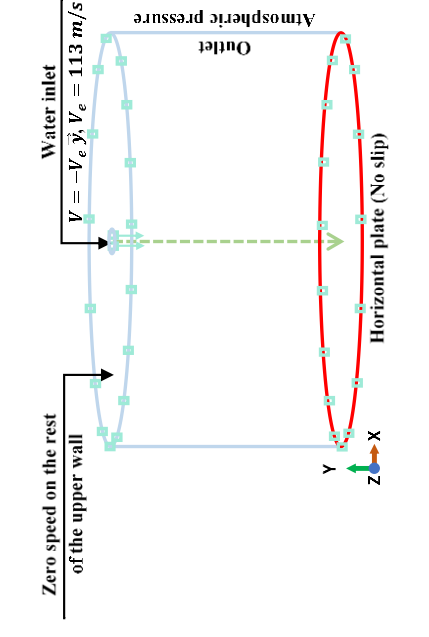
<p>Geometric formulation</p>  <p>Nozzle outlet</p> <p>Water jet</p> <p>Plate target level</p> <p>\vec{V}_e</p> <p>H</p> <p>L</p> <p>\vec{U}_r</p>	<p>Fluid volume and boundary conditions</p>  <p>Water inlet</p> <p>$V = -V_e \hat{y}$, $V_e = 113 \text{ m/s}$</p> <p>Outlet</p> <p>Atmospheric pressure</p> <p>Zero speed on the rest of the upper wall</p> <p>Horizontal plate (No slip)</p> <p>x, y, z</p>
<p>jet Parameters</p> <ul style="list-style-type: none"> • the velocity magnitude at the exit of the nozzle • $V_e = 113 \text{ m/s}$ The nozzle diameter $D = 1 \text{ mm}$ • The distance of separation (DOS) between the outlet of the nozzle and the target: $H = 10D$; • Target radius $R = 12D$. 	<p>turbulence Modelling</p> <ul style="list-style-type: none"> • Reynolds number: $Re = 113000$; • Turbulence model: RNG $k - \epsilon$; • The initial value of the turbulent kinetic energy k_0 as well as of the turbulent dissipation ϵ_0 are given by the following equation: $\begin{cases} k_0 = 0,002 V_e^2 \\ \epsilon_0 = \frac{k_0^{1.5}}{0.3 D} \end{cases}$
<p>hypothesis</p> <ul style="list-style-type: none"> • The water flow is considered three-dimensional, weakly compressible, turbulent and stationary on average; • The density is assumed to be independent of time; • a cylindrical coordinate system is adopted • We will not consider the thermal aspect; therefore, the resolution of the fluid problem is done at a constant temperature. 	

Table 2: Physical properties of fluid water.

Water density	$\rho = 1000 \text{ kg m}^{-3}$
Dynamic viscosity	$\mu = 10^{-3} \text{ Pa s}$
EOS	U_s-U_p
sound Reference speed in water	$C_0 = 1450 \text{ m/s}$
Slope of the US-Up curve	$s = 0$
Grüneisen Constant	$\Gamma_0 = 0$

4 Numerical results

4.1- Mesh and dependency grid

within this CFD study, we tried to create a well-adapted mesh: Enough high density to faithfully reproduce the details of the geometry but with a limited number of meshes so as not to unnecessarily slow down the calculation. we generated a hybrid mesh composed of form elements (FC3D6: Prism with six nodes and FC3D8: Brick with eight nodes). After introducing the inlet geometry, this volume would have significant geometric transitions. Thus, in order to ensure a good and fast convergence, the mesh refinement was carried out in the inlet nozzle and the target as presented in the following figure 5. As far as the mesh was refined, we considered the smoothing transition. Then, we varied the number of elements on the borders adjacent to the refinement areas. In this CFD analysis, we adopted the maximum pressure on the target as a criterion to follow the grid dependency. Figure 6 shows the mesh sensitivity of the maximum pressure as a function of time. Notice here that from an optimal density, the pressure evolves almost independently of the mesh. This density has been established at a number of approximately one million meshes ($N_{opt} = 1054861$).

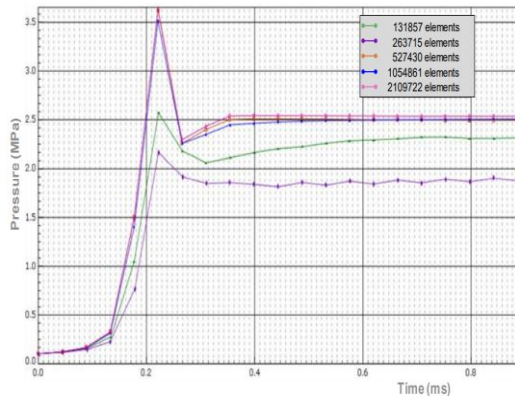


Figure 6: Mesh sensitivity: Maximum pressure on the target.

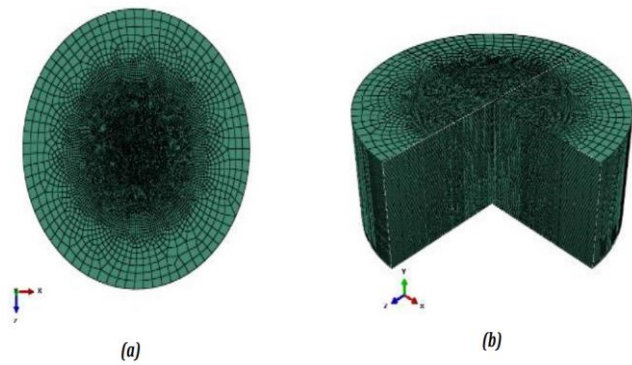


Figure 5: Discretization of a) of the target b) the entire volume of fluid.

4.2- The velocity's profile

Figure 8 shows the velocity profile of the jet at the final moment. Morphologically, this profile has an almost cylindrical shape just at the near outlet of the nozzle. When propagated towards the target, the flow takes a bell shape and can be subdivided into three main regions. After a flow time of approximately 0.176ms in the surrounding volume, the structure of the free (or autonomous) jet is fully established as presented in figure 9. This region will be retained until the end of the flow. Such result is shown and detailed in several references [24], [25], [26], [1], [27] and [28] spotting on jet dynamics. The choice of the distance between the nozzle and the structure to be impacted, which is

$H = 10$, made it possible to observe this jet structure [1]. The freestream dynamic begins to develop immediately as the water exits to the surrounding volume. Indeed, near the opening of the nozzle, a

mixing zone arises and a turbulent mass diffusion takes place. Figure 10 shows the appearance of already turbulent primary structures observed at **0.08** from the nozzle.

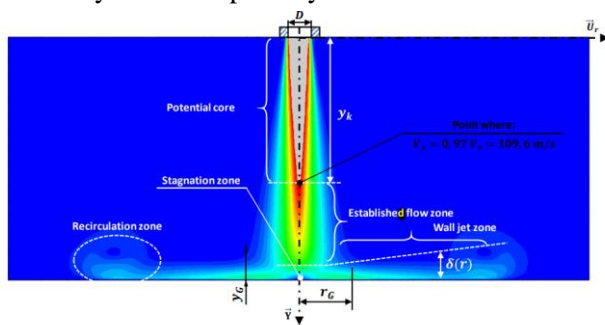


Figure 8: Velocity profile at the final moment $t_f = 10 T$.

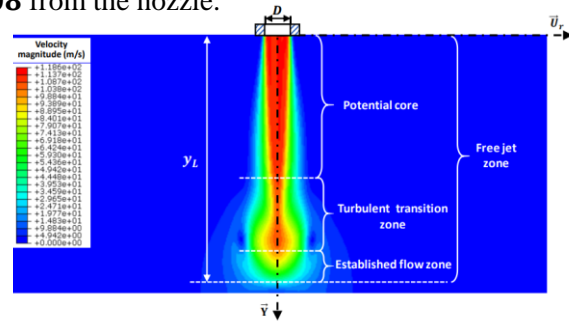


Figure 9: Velocity profile at moment $t = 2T$.

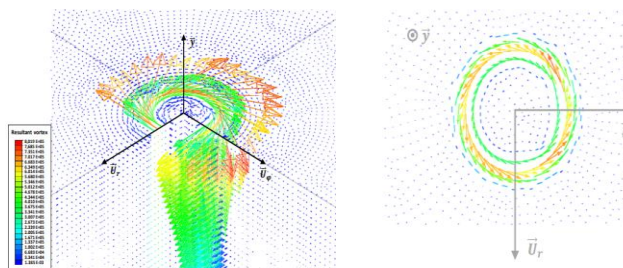


Figure 10: Vorticity at 0.08 mm from the nozzle outlet.

The incident jet may be considered a free jet except in the immediate vicinity of the impact surface. In this simulation, the free jet region extends from the nozzle to a distance equal to $y_L = H - y_G = 8.64 \text{ mm}$ (as highlighted in figure 9).

The actual potential length of the core corresponds to the distance between the virtual origin of the jet and the point where the central velocity of the jet begins to decrease. Figures 8 and 11 show that the centerline velocity is reduced to 97% regarding the velocity at the nozzle inlet when moving away from the distance $y_k = 6.1 \text{ mm}$ from the jet origin. The stagnation zone extends at a distance « » from the target. Figure 12 shows the deviation of the axial velocity measured numerically at = **1, 3** mm

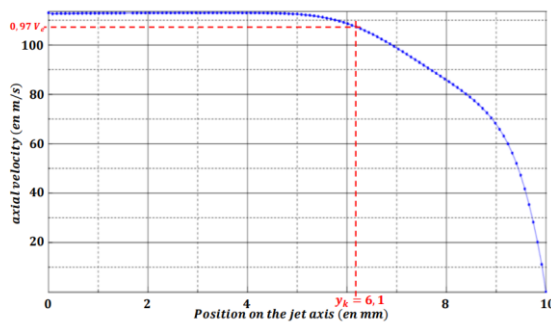


Figure 11: The centerline velocity at $t = 10 T$.

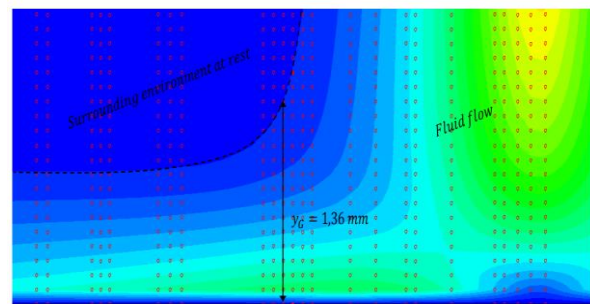


Figure 12: The velocity profile in the near neighbor of the target at $t = 10 T$.

Figure 13 shows the evolution of the axial component of the velocity at different heights « h » from the target at the final moment t_f . These curves show that the closer one gets to the target (at $h = 0$) the lower centerline velocity. This decrease is also observed when moving away from the centerline of the jet. All velocities taking a zero value or almost at a common point located at a radius $r_G = 0,55 \text{ mm}$ marking thus the end of the stagnation zone. Figure 14 shows the thickness of the boundary layer in the immediate neighbor of the target. This layer mentions the stall area of the flow. The numerical simulation shows a thickness equal to $\delta_0 = 0.38 \text{ } 10^{-3} \text{ mm}$. Among all simulation results, this measurement is the furthest from the analytical value. Indeed, as shown in figure 14, the cell length is larger than this physical size. Therefore, the mesh does not allow representing in a satisfactory way. The results shown in the following Table 3 show a good and satisfactory correlation between the characteristic values of the velocity profile analytically calculated and numerically obtained.

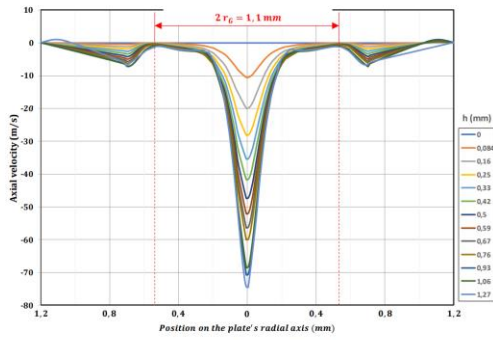


Figure 13: Centerline velocity at different heights from the target at $t = 10 T$.

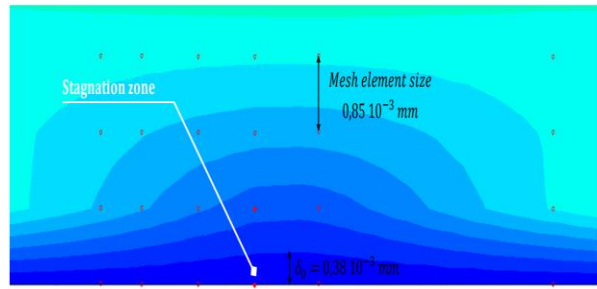


Figure 14: Minimum thickness in the boundary layer: Within the stagnation zone at $t = 10 T$.

Table 3: Comparison between analytical and numerical studies.

Characteristic length	Designation	Analytical value (mm) « V_A »	Numerical value (mm) « V_N »	Relative error $\epsilon = \frac{V_A - V_N}{V_A}$ (%)
Core zone length	y_k	$4 \leq y_k \leq 7,7$	6,1	$21 \leq \epsilon \leq 53$
Stagnation zone length	y_G	1,2	1,36	13
Radius of the stagnation zone	r_G	0,62	0,55	11
Minimum thickness of the boundary layer	δ_0	$6,93 \cdot 10^{-3}$	$0,38 \cdot 10^{-3}$	95

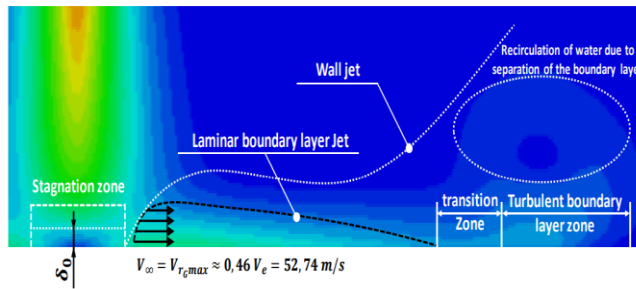


Figure 15: Wall jet region structure at t_f .

Figure 15 illustrates the three different regions forming the wall jet area at the flow's final moment. These three regions are associated with different flow regimes: A laminar boundary layer, a transient boundary layer and a turbulent boundary layer

4.3 Pressure Distribution on the target

The pressure in the potential core region is almost constant. It is equal to the pressure of the surrounding environment and it is about $0.14 Pa$. In this area, the pressure variation is inconsiderable in the direction of flow. As a result, the effect of a pressure gradient in the potential core area is relatively small in terms of flow propagation. The pressure gradient starts to be significant at the beginning of the stagnation zone, i.e. $y = yL$. The pressure reaches a maximum value at the central stagnation point. This value is about $2.54 Pa$.

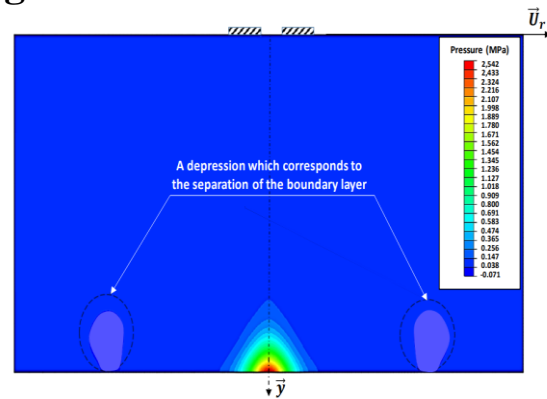


Figure 20: Pressure distribution cross the symmetry plane $(0, \vec{y}, \vec{U}_r)$ of the studied volume at the final moment t_f .

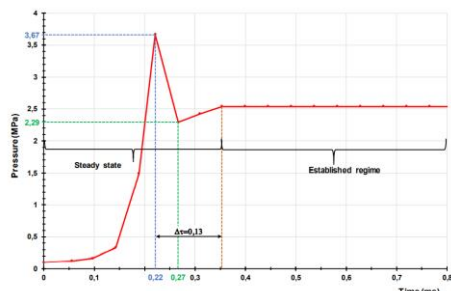


Figure 22: History of maximum pressure variation at the center of the plate during $10 T$.

The so-called « τ » is denoted as the required time to reach the first point of the obstacle, which is the center of the circular target. This time is approximately $2,5 T$: $\tau = 2,5 T$. This is illustrated by a pressure peak in Figure 22, which represents the maximum pressure time evolution regarding the time at the center of the obstacle.

5- CONCLUSION

In this study the capability of a CFD modeling approach is evaluated. this CFD analysis is carried out with the aim to model a water jet impacting a circular and fixed target. The water flows from a circular nozzle at a constant velocity of 113m/s. The nozzle/plate separation distance is 10 times the nozzle diameter. A comparison was made with an analytical / empirical study presented in references [1] and [20]. The numerical CFD model built presents very good correlations in terms of the velocity profile. Regarding the pressure field, the CFD model gives a quantitative and qualitative idea of the distribution of pressure on the target after a sufficiently long duration of the water flow in the studied volume. Thus, the present study allowed us to calibrate the model and to control the methodology of the calculations. We also familiarized with the Abaqus software and the various numerical steps required in building a «simple» modeling of the impacting axisymmetric jet dynamics. It would be very interesting to study the pressure considering the fluid coupling structure. This will be the subject of further study

References

- [1] H. MARTIN, 1977. Heat and mass transfer between impinging gas jets and solid surfaces *Advances in Heat Transfer*, 13, 1-60.
- [2] M. Kaushik, S. Kumar, and G. Humrutha, 2015. Review of computational fluid dynamics studies on jets, *American journal of fluid dynamics* 5(a), 1–11.
- [3] C. Y. Hsu, C. c. Liang, T. L. Teng and A. T. Nguyen, 2013. A numerical study on high speed water jet impact, *ocean engineering*, 72,98–106.
- [4] M. Chizari, S. T. S. Al-hassani and L. M. Barrett, 2008. Experimental and numerical study of water jet spot welding, *journal of materials processing technology*, 198(1–3), 213–219.
- [5] M. Chizari, L. M. Barrett and S.T.S. Al-hassani, 2009. An explicit numerical modelling of the water jet tube forming, *computational materials science*, 45(2), 378–384.
- [6] T. Mabrouki, K. Raissi and A. Cornier, 2000. Numerical simulation and experimental study of the interaction between a pure high-velocity waterjet and targets: Contribution to investigate the decoating process, *wear*. 239- 260.
- [7] T. Mabrouki, K. Raissi, 2002. Stripping process modeling: Interaction between a moving waterjet and coated target, *int. J. Machi. Tool. Manuf.* 42, 1247.
- [8] A. Saxena and O. Paul, 2007. Numerical modeling of kerf geometry in abrasive water jet machining, 2007, *int. J. Abras. Techo.* 1, 208.
- [9] Y. Ayed, C. Roberta, G. Germaina and A. Ammara, 2016. Development of a numerical model for the understanding of the chip formation in high-pressure water-jet assisted machining, *fin. Elem. Anal. Des.* 108, 1.
- [12] H. Schrader, 1961. Trocknung feuchter Oberflächen mittels Warmluftstrahlen. Strömungsvorgänge und Stoffübertragung. *VDI Forschungsheft* 484 (1961).
- [13] H. Glaser, 1962. Untersuchungen an Schlitz- und Mehrdüsenanordnungen bei der Trocknung feuchter Oberflächen durch Warmluftstrahlen, *chemi Ingenieur technik*, 34, 200 (1962).
- [14] R. Lohe, 1983. Berechnung und Ausgleich von Kräften in räumlichen Mechanismen. *Fortschr.-Ber. VDI-Z., Reihe 1, Nr. 103* (1983).
- [15] P. N. Romanenko and I.S. Verigin, 1970. Effect of the transverse mass flow on the heat exchange and dynamics of a stream in turbulent heated air flow in an axisymmetric diffusor with a permeable wall, *Journal of Engineering Physics*, 19, 924–928 <https://doi.org/10.1007/BF00828760>.
- [16] M. Glauert, 1956. The wall jet. *Journal of Fluid Mechanics*, 1(6), 625-643. doi:10.1017/S002211205600041X).

- [17] S. Goldstein, 1939. A note on the boundary layer equations. *Mathematical Proceedings of the Cambridge Philosophical Society*, 35 (2), 338-340. doi:10.1017/S0305004100021046.
- [18] Abramovich and N. Genrikh, 1963. *The theory of turbulent jets*. Mit press, 1963.
- [19] E. U. Schliinder, 1971. Wärmeübergang an bewegte Kugelschüttungen bei kurzfristigem Kontakt chemi ingenieur technik. 19, 108, <https://doi.org/10.1002/cite.330431103>.
- [20] J. W. GuzIntner, J. N. B. Livingood and P. Hrycuk, 1970. Survey of literature on flow characteristics of a single turbulent jet impinging on a flat plate. Technical Note, NASA TECHNICAL NOTE, NASA TN D-5652.
- [21] G. A. Dosdogru, 1972. Einfluß des Turbulenzgrades auf den Wärme- und Stoffübergang in Schlitzdüsen, *Chemie Ingenieur Technik*, 44, 1340
- [22] W. Schwarz and W. Cosart (1961). The two-dimensional turbulent wall-jet. *Journal of Fluid Mechanics*, 10 (4), 481-495. doi:10.1017/S0022112061000299.
- [23] P. Bakke, 1957. An experimental investigation of a wall jet. *Journal of Fluid Mechanics*, 2 (5), 467-472. doi:10.1017/S0022112057000270.
- [24] T. Dairay, V. Fortune, E. Lamballais, L.-E. Brizzi, 2010. Simulations Numériques Directes d'un jet impactant, Conference paper, 20eme Congres Français de Mécanique, Besançon.
- [25] J. Hamdi, 2017. Reconstruction volumique d'un jet impactant une surface fendue à partir de champs cinématiques obtenus par piv stéréoscopique. *Mécanique des fluides [physicsclass-ph]*. Université de la rochelle, 2017. Français. Ffnnt: 2017laros027ff. Fftel 01804959f.
- [26] B. LeBlanc, 2016. Etude aérodynamique d'un jet turbulent impactant une paroi concave. 2016, Maîtrise Ès Sciences Appliquées, Université de Moncton.
- [27] Y. Le Guer, 2005. Jet confiné, dispersions fluide-particules et mélange chaotique. *Sciences de l'ingénieur [physiques]*. Université de Pau et des pays de l'Adour, 2005.
- [28] P. AILLAUD, F. DUCHAINE, L. GICQUEL, Analyse aérothermique d'un jet circulaire impactant sur plaque plane à l'aide de la SGE, Centre européen de recherche et de formation avancée en calcul scientifique (CERFACS), Equipe CFD.